

# Stochastic molecular motions in the nematic, smectic-A, and solid phases of *p,p'*-di-*n*-heptyl-azoxybenzene as seen by quasielastic neutron scattering and $^{13}\text{C}$ cross-polarization magic-angle-spinning NMR

Wojciech Zając\*

*The H. Niewodniczański Institute of Nuclear Physics, Polish Academy of Sciences, Radzikowskiego 152, 31-342 Kraków, Poland*

Stanisław Urban

*Institute of Physics, Jagiellonian University, Reymonta 4, 30-059 Kraków, Poland*

Valentina Domenici, Marco Geppi, and Carlo Alberto Veracini

*Dipartimento di Chimica e Chimica Industriale, Università degli Studi di Pisa, via Risorgimento 35, 56126 Pisa, Italy*

Mark T. F. Telling

*ISIS Facility, Rutherford Appleton Laboratory, Chilton, Didcot OX11 0QX, United Kingdom*

Barbara J. Gabryś

*Department of Materials Science, University of Oxford, Parks Road, Oxford OX1 3PH, United Kingdom*

(Received 12 October 2005; published 11 May 2006)

Molecular rotational dynamics in *p,p'*-di-*n*-heptyl-azoxybenzene was studied by means of quasielastic neutron scattering (QENS) and  $^{13}\text{C}$  cross-polarization magic-angle-spinning (CPMAS) NMR. Fast reorientation of the hydrogen nuclei was observed by QENS in the two liquid crystalline (LC) phases nematic and smectic A, as well as in the crystalline phase. The latter could not be restricted to the  $-\text{CH}_3$  rotations alone, and a clear indication was found of some other reorientation motions persisting in the crystal. Two Lorentz-type components convoluted with the resolution function gave an excellent fit to the QENS spectra in both LC phases. The narrow (slow) component was attributed to the reorientation of the whole molecule around the long axis. The corresponding characteristic time of  $\sim 130$  ps agreed well with the values obtained in recent dielectric relaxation and  $^2\text{H}$  NMR studies. The full width at half maximum of the broader (fast) component shows a quadratic  $Q$  dependence ( $Q$  is the momentum transfer). Hence the corresponding motions could be described by a stretched exponential correlation function and were interpreted as various “crankshaft-type” motions within the alkyl tails. The  $^{13}\text{C}$  CPMAS experiments fully corroborated the QENS results, sometimes considered ambiguous in complex systems.

DOI: [10.1103/PhysRevE.73.051704](https://doi.org/10.1103/PhysRevE.73.051704)

PACS number(s): 61.30.-v, 61.12.Ex, 67.80.Jd, 67.40.Fd

## I. INTRODUCTION

The understanding of rotational dynamics in liquid crystalline (LC) phases is still far from being complete, despite many years of intensive work. The interest in liquid crystals is due to both fundamental problems as well as practical ones, i.e., the search for new, better LC displays. The high anisotropy of liquid crystalline systems creates a specific environment for the rotations of whole molecules (Refs. [1–6]).

Rodlike LC molecules in the nematic phase can rotate around their principal axes of inertia and with respect to the director. Four such motions were described theoretically [1–4] and have been found by tailor-made experiments (for example, Refs. [3,4,6]). In addition, complex chemical structures of these molecules result in a variety of intramolecular motions, such as conformational kinks in the lateral alkyl or alkoxy chains, and the rotations of larger molecular fragments around single bonds. The complexity of these motions is aggravated, on one hand, by the fact that they occur on

very different time scales, ranging from seconds to picoseconds, and, on the other hand, by possible dynamical coupling with intramolecular vibrations. While some corresponding relaxation processes are well separated in the frequency domain, other processes overlap, which makes it difficult to separate them in the measured spectra. Hence it is impossible to study or detect all such motions by means of one experimental technique.

A wealth of experimental methods has been applied to study molecular dynamics in liquid crystals so far (for example Refs. [5,7–10]). Particular spectroscopic methods are characterized by their own time windows and are sensitive to the specific molecular quantity (dipole moment, atom-atom vector, radius of rotation) [11]. Moreover, some methods mostly give a single-molecule response (such as those particular ones applied in this work), whereas dielectric spectroscopy is a polymolecular one. One has to bear this in mind while comparing values of, e.g., relaxation times obtained by different methods. Ideally, several complementary techniques ought to be used to study one sample in order to eliminate ambiguities in data analysis.

\*Electronic address: Wojciech.Zajac@ifj.edu.pl

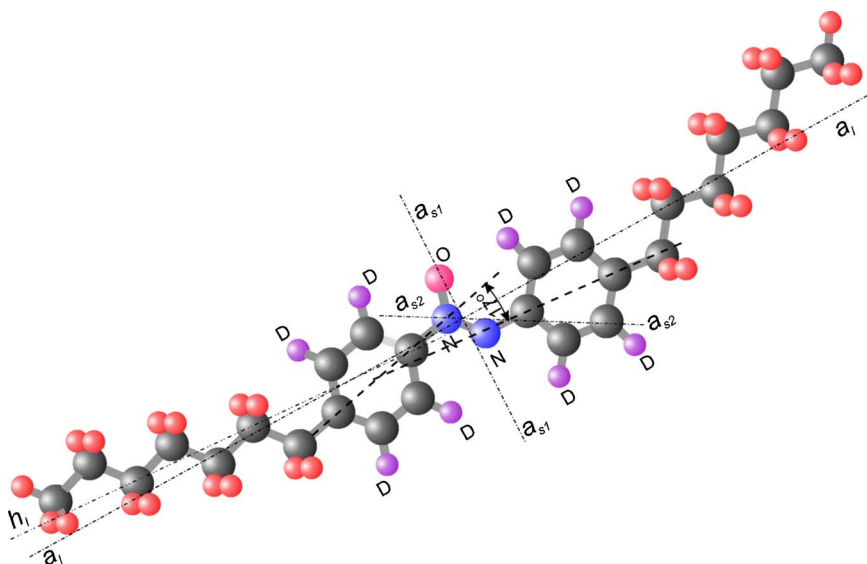


FIG. 1. (Color online) The structure of the HAB molecule. D denotes deuterium atoms in ring-deuterated ( $d_8$ ) samples. C and H atoms are not labeled for clarity. The  $p$  axes of the benzene rings form an angle of  $17^\circ$  (Ref. [15]). Indicated are benzene  $p$  axes, principal inertia axes of the molecule,  $a_1$ - $a_3$ ,  $a_{s1}$ - $a_{s3}$ ,  $a_{s2}$ - $a_{s4}$ , and the long inertia axis of the left “half” of the molecule,  $h_1$ - $h_l$ .

In the present paper we present an in-depth analysis of the rotational dynamics in  $p,p'$ -di- $n$ -heptyl-azoxybenzene (HAB or 7AOB). Between crystal and isotropic phases, this substance exhibits a liquid crystalline polymorphism with the nematic ( $N$ ) and smectic- $A$  ( $S_A$ ) phases. The results obtained by means of quasielastic neutron scattering (QENS) are confirmed by a  $^{13}\text{C}$  cross-polarization magic-angle-spinning (CPMAS) study, and compared to those obtained by dielectric spectroscopy [6,12,13] and nuclear magnetic resonance (NMR) [13–15].

The shape of a free HAB molecule, shown in Fig. 1, is the one that optimizes its geometry. Note that the dipole moment created by the azoxy group is rather rigidly coupled to the molecular core. Therefore dielectric relaxation studies give reliable results as to overall molecular motions around the principal inertia axes: the low frequency process yields information about tumbling of the molecule around its short axis, while the high frequency process that about its spinning around the long axis. Moreover, the precession of the long axis around the director might lead to a separate relaxation process. The relaxation time characteristic for the low frequency process,  $\tau_{0,0}^1$ , is of the order of  $10^{-7}$  s in the  $N$  phase and  $10^{-6}$  s in the  $S_A$  phase with the activation enthalpies  $\Delta H_{lf}$  equal to 100 and 60 kJ/mol, respectively [6,12,13]. For the high frequency process we have  $\tau_{1,1}^1$  of the order of  $10^{-10}$  s and  $\Delta H_{hf}=25$  kJ/mol in both phases [12,13].

The selectively deuterated HAB molecule (both benzene rings and two adjacent protons in the alkyl tails) was studied previously by  $^2\text{H}$  NMR techniques, which yielded information about structural and ordering behavior [15] as well as about overall and internal motions [13,14]. It was established that, besides the tumbling and spinning motions, the benzene rings perform independent rotation around their  $p$  axes with dynamical parameters not far from those of the spinning motion. The diffusion coefficients  $D_\perp$  and  $D_\parallel$  obtained from the NMR spectra are not directly comparable to the dielectric relaxation times. In order to be able to compare the two, one has to derive the correlation times from the NMR  $D_\perp$  and  $D_\parallel$  using quantities such as the nematic order parameter [16–18]. Once this was done, a full consistency was

achieved between the dielectric relaxation times, which are macroscopic values, and the microscopic NMR correlation times, in both liquid crystalline phases of HAB [13].

Such an agreement between the results of two experimental methods might be fortuitous only for the reasons mentioned above. This is why it was deemed desirable to employ yet another spectroscopic method, namely, quasielastic neutron scattering, aimed at providing complementary information on inter- and intramolecular reorientations. The results obtained were compared with previously reported  $^2\text{H}$  NMR and dielectric relaxation results, as well as with those arising from  $^{13}\text{C}$  cross-polarization magic-angle-spinning experiments, carried out in both mesophases and in the solid state as reported in the present paper. Indeed, the  $^{13}\text{C}$  spectra could be interpreted in terms of conformational and dynamic behavior of either of the aromatic and aliphatic HAB moieties, therefore complementing the interpretation of QENS data. To our knowledge, this is a first time a combination of the QENS and  $^{13}\text{C}$  CPMAS techniques has been used to investigate motions in liquid crystals.

## II. QUASIELASTIC NEUTRON SCATTERING

Quasielastic neutron scattering is a high resolution incoherent inelastic neutron scattering in the close proximity of the elastic line. It is sensitive to relatively fast stochastic motions of the scattering nuclei (rotation, libration, diffusion, etc.) Due to the large incoherent scattering cross section of the proton<sup>1</sup> the main contribution to the scattered intensity arises from the hydrogen atoms in the molecule, and the selective H:D isotope substitution is commonly used to highlight the scattering due to certain parts of the sample.

In the time window of quasielastic neutron scattering, molecular vibrations will only affect the spectrum through the Debye-Waller factor:  $\exp(-\langle u^2 \rangle Q^2)$ , where  $\langle u^2 \rangle$  is the mean-square displacement of the scattering center, and  $Q$  is the momentum transfer. Moreover, in solid and liquid crystalline

<sup>1</sup> $\sigma_H^{inc}=80$  b;  $1$  b= $10^{-28}$  m<sup>2</sup>.

phases translational diffusion is far too slow to be detected by QENS; hence it does not enter into our analysis. Therefore, the QENS signal we can see is due to a number of rotation-type reorientations. If (and only if) the latter are dynamically independent, the scattering law  $S_{inc}(Q, \omega)$  ( $\hbar\omega = E - E_0$  is the energy transfer) is a convolution of scattering laws connected with each such reorientation:

$$S_{inc}(Q, \omega) = \exp(-\langle u^2 \rangle Q^2) \times S_1(Q, \omega) \otimes \cdots \otimes S_n(Q, \omega). \quad (1)$$

For a motion confined in space  $S_{inc}(Q, \omega)$  contains an elastic contribution, and for a simple rotation it takes the following form:

$$S_{inc}(Q, \omega) = A(Q)\delta(\omega) + [1 - A(Q)]L(\omega, \Gamma), \quad (2)$$

where  $L(\omega, \Gamma)$  is a Lorentzian with the full width at half maximum (FWHM) equal to  $\Gamma$ .  $L(\omega, \Gamma)$  arises as a Fourier transform of this form of the time-dependent part

$$I'_{inc}(Q, t) \propto \exp\left(-Q^2 \frac{t}{\tau}\right) \quad (3)$$

of the intermediate scattering function. Here  $\tau$  is the *characteristic time* of a given type of motion, e.g., for stochastic jumps over equidistant sites on a circle, this will be a mean residence time in one position.

It can be seen from Eq. (2) that  $S_{inc}(Q, \omega)$  depends upon  $Q$  only through the amplitude  $A(Q)$ . Since the time characteristic of the motion under study is expressed by the linewidth, the spatial characteristic can be deduced from the elastic incoherent structure factor (EISF):

$$\text{EISF}(Q) = \frac{I_{el}(Q)}{I_{el}(Q) + I_{inel}(Q)}. \quad (4)$$

Rodlike molecules of liquid crystals exhibit stochastic rotational reorientation around their long and short axes as well as independent reorientation of molecular “halves” (cf. Fig. 1) [9,19–21]. Reorientation around the short axis of an elongated molecule will hardly be visible in a QENS experiment, as it occurs on a much too slow time scale. In order to detect very fast reorientations within the alkyl chains, while slower motions are also active, a finely tuned instrument is necessary,<sup>2</sup> and great care needs to be taken during data analysis and interpretation.

Most QENS experiments on rodlike liquid crystals performed so far in the smectic and nematic phases could be safely interpreted in terms of rotation of the whole molecule and, if applicable, its parts defined by an atomic group bridging the benzene rings. Slightly faster motions were usually considered to contribute to the background and were thus not visible. Technical improvement in the instrument design and a precise temperature control make it possible to see the influence of a variety of motions on the QENS spectra. The main question now is whether and to what extent the reori-

entation of the whole molecule and/or its “halves” still dominates the spectrum, not only in terms of contribution to the scattered intensity but also in terms of the spectrum dependence on the momentum transfer. One can proceed by assuming certain models of reorientation, calculating scattering laws, and least-squares fitting their parameters to the data. This would result in a large number of free parameters and an inability to discriminate between such models. Therefore a reverse formulation of the problem seems methodologically better, namely, what is the number of quasielastic components we have the most evidence for, given the experimental data at hand? This formal probabilistic reasoning within the *Bayesian* approach to data analysis can be applied for QENS:

$$\Pr(N|\{\text{data}\}) \propto \Pr(\{\text{data}\}|N) \times \Pr(N). \quad (5)$$

Here  $\Pr(N|\{\text{data}\})$  represents the *posterior probability distribution*, and  $\Pr(N)$  is the *prior*.  $\Pr(\{\text{data}\}|N)$  can be calculated as a model scattering law for a given type of motion.

To be precise, this method, as implemented for QENS [22], allows one to conclude what is the most likely number of Lorentzian components in the spectrum, rather than quasielastic components in the scattering law. The difference can be seen, e.g., from Eq. (1). A combination of, say, two rotations results in three Lorentzian components:

$$S_1(Q, \omega) \otimes S_2(Q, \omega) = A\delta(\omega) + BL(\omega, \Gamma_1) + CL(\omega, \Gamma_2) + DL(\omega, \Gamma_1 + \Gamma_2). \quad (6)$$

### III. EXPERIMENT

The  $d_0$ -HAB samples were the same as in previous studies (Refs. [12–15]). Instead of  $d_{12}$ -HAB used in Refs. [12–15],  $d_g$ -HAB was synthesized following the procedure described by Van der Veen *et al.* [23].

The QENS experiment was performed at the ISIS Neutron Spallation Source, Rutherford Appleton Laboratory using the OSIRIS backscattering crystal-analyzer spectrometer. This is an “inverted geometry” instrument with pyrolytic graphite energy analyzers, which are cooled down to ca. 8 K. The latter were set to the (002) reflection (neutron wavelength  $\langle \lambda \rangle = 6.69 \text{ \AA}$ ). In these conditions, the instrument energy resolution can be estimated as  $25 \mu\text{eV}$ , and the accessible momentum transfer range is  $0.2 < Q < 1.8 \text{ \AA}^{-1}$  (cf. Ref. [24]).

A standard flat aluminum sample can was used,  $2 \times 4 \text{ cm}^2$ , and 0.3 mm deep. Such a thin sample ensured that the multiple scattering effects were negligible (subsequently checked by Monte Carlo simulation), yet retaining a good counting rate. A liquid nitrogen cryostat with a precise temperature controller provided good temperature stabilization, particularly important in the vicinity of phase transition points.

The spectra for both hydrogenous and ring-deuterated samples were collected at 280 K (crystalline phase), at 317, 322, 327 K (smectic phase), and at 337, 341, 344 K (nematic phase). The above mentioned  $Q$  range was covered by simultaneous data acquisition at different scattering

<sup>2</sup>That is, producing “clean” spectra, free from spurious effects, thermodiffusion broadening by the analyzers, etc., such as the OSIRIS spectrometer at ISIS, RAL.

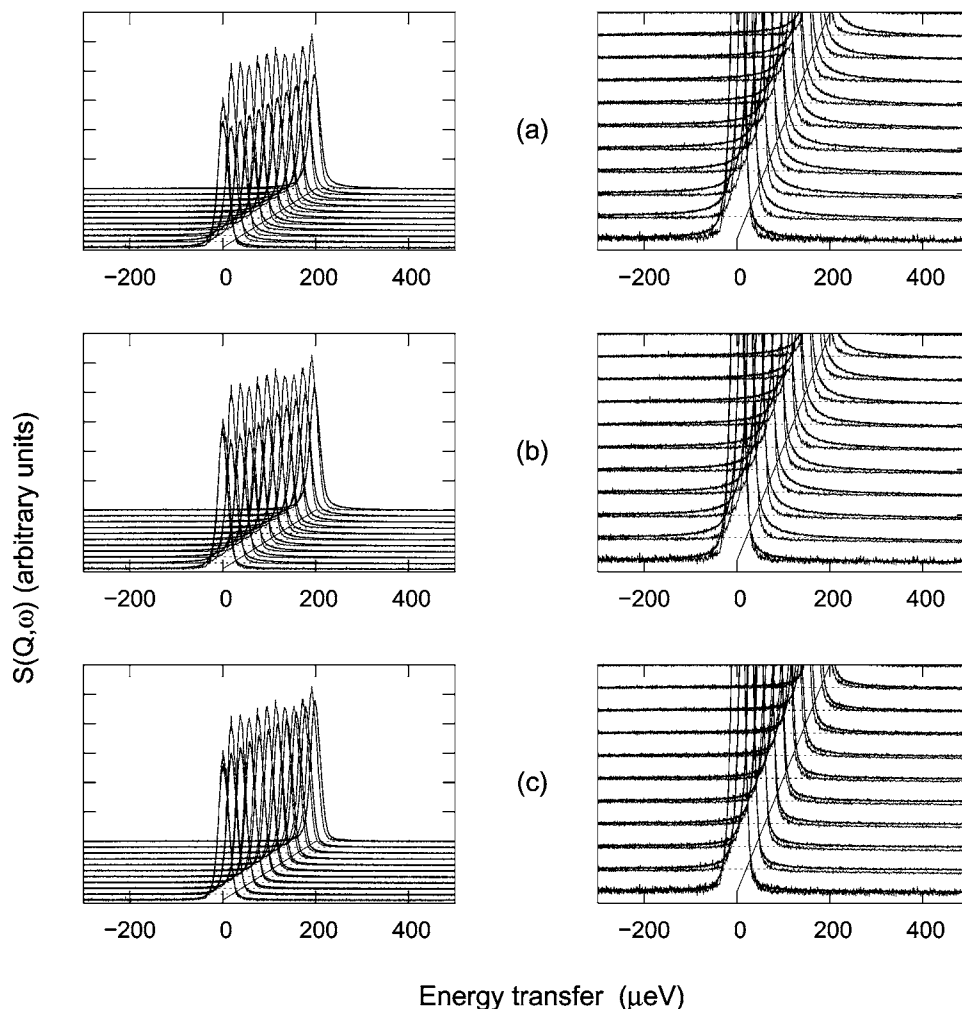


FIG. 2. Typical QENS spectra shown together with the instrument resolution function (vanadium elastic line) for several values of momentum transfer. The right column presents enlarged bottom parts of the same spectra as the left one. (a):  $d_8$ -HAB nematic at 341 K, (b)  $d_8$ -HAB smectic at 322 K, and (c)  $d_8$ -HAB crystal-line at 280 K.

angles. The spectra were subjected to standard data reduction procedures such as correction for self-absorption, background subtraction, etc., by instrument-specific code working under the Open GENIE environment. Assuming Lorentzian components, the problem of finding the “most likely” number of lines is solved by the appropriate software module incorporated into the MODES package [25], made accessible to ISIS users. In all cases, except the crystal phase, the answer was two Lorentzian components. Since the widths of component lines differ by at least an order of magnitude, we can safely conclude that this also means two quasielastic components. Vanadium elastic lines were taken as the instrument resolution function. HAB spectra collected in the crystalline phase could not serve this purpose as some reorientation processes are still active in the crystalline phase at 275 K (see discussion below).

$^{13}\text{C}$  CPMAS experiments were carried out on a double-channel Varian Infinity Plus 400 spectrometer, working at 100.56 MHz for  $^{13}\text{C}$ , equipped with a 7.5 mm CPMAS probe. The sample was put within a glass ampoule fitting the  $\text{ZrO}_2$  rotor, and sealed by an epoxy glue. The spectra were recorded by spinning the sample at the magic angle ( $54.74^\circ$ ) with respect to the external magnetic field with a spinning frequency of 3 kHz, and under high power  $^1\text{H}$ -decoupling conditions, realized by means of the SPINAL-64 pulse se-

quence [26]. The CP conditions were achieved using a linear ramp on the carbon channel.  $^1\text{H}$  and  $^{13}\text{C}$   $90^\circ$  pulse lengths were  $4.3 \mu\text{s}$ . 600 scans were accumulated in the nematic and smectic-A phases, and 3600 scans in the solid phase. Temperature was always controlled within 0.2 K.

#### IV. RESULTS

Typical QNS spectra collected in the nematic, smectic-A, and crystalline phases of the ring-deuterated (“ $d_8$ ”) sample are presented in the left column of Fig. 2. Narrow lines are the elastic incoherent vanadium spectra, treated as the instrumental function, whereas thick lines are the measured spectra. Both the vanadium and HAB spectra were normalized to the same area. In order to display the quasielastic broadening more explicitly the bottom parts of the spectra were enlarged and presented on the right hand side. Spectra of three phases of  $d_8$ -HAB at the midpoint of the  $Q$  scale are shown in Fig. 3 for comparison.

A selection of  $^{13}\text{C}$  CPMAS spectra recorded in the nematic, smectic-A, and solid phases of HAB is reported in Fig. 4. The assignment of the signals has been carried out on the basis of the solution state spectrum. In the following discussion we will refer to the spectrum recorded at  $60^\circ\text{C}$  (nematic phase), and to a labeling obtained by numbering the

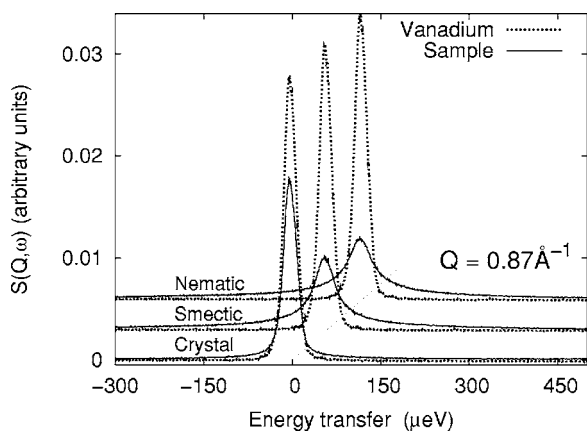


FIG. 3. Scattering law versus energy transfer recorded at one  $Q$  value (i.e., the same scattering angle) in the three phases of HAB and compared with the incoherent elastic spectrum of vanadium. The spectra were normalized to the same areas. Quasielastic broadening increases with the increasing temperature. Note that already in the solid phase at 275 K a clear broadening is observed, which cannot be attributed solely to the reorientation of the  $\text{CH}_3$  end groups.

aliphatic chain carbons from 1 to 7 going from the methyl group to the methylene bonded to the aromatic ring. The peaks at 14.7, 23.4, and 36.5 ppm are ascribed to C1, C2, and C7, respectively, while the group of resonances in the region 29–34 ppm is due to “internal” chain carbons C3–C6. The aromatic carbons give rise to two groups of signals in the regions 140–150 ppm (quaternary carbons) and 120–130 ppm (tertiary carbons).

## V. DISCUSSION

### A. QENS results

Excellent quality fits of two-component scattering law to the spectra were obtained. As seen from, e.g., Eq. (2), the linewidths resulting from such fits should not depend upon

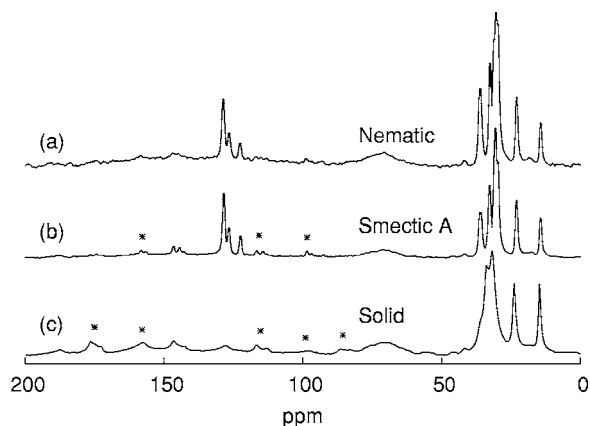


FIG. 4.  $^{13}\text{C}$  CPMAS spectra of HAB recorded in the nematic (60 °C), smectic-A (45 °C), and solid (21 °C) phases under  $^1\text{H}$  high power decoupling conditions and the sample spinning frequency of 3 kHz. Asterisks denote spinning sidebands. The signal at about 70 ppm is due to the epoxy glue.

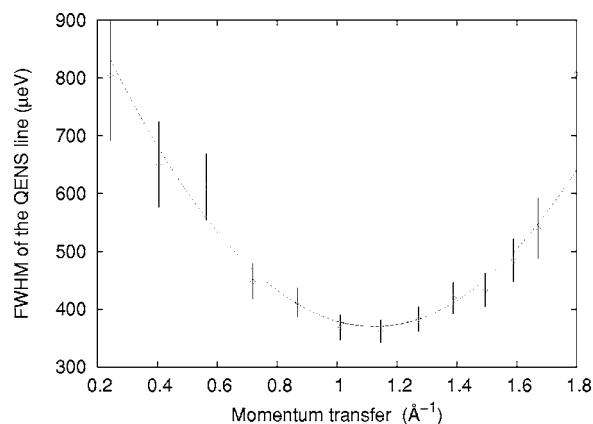


FIG. 5.  $Q$  dependence of the linewidth of the broader QENS component. It appears to be quadratic with minimum around the scattering angle  $\theta=75^\circ$ . This scattering angle is by no means specific. There is no apparent reason for this kind of behavior since we are dealing with rotational type of motions without any, e.g., translational diffusion.

momentum transfer beyond the statistical uncertainties. The narrow component is almost constant in width ( $\langle\text{FWHM}\rangle \cong 40 \mu\text{eV}$ ), whereas the broader one shows a clear and systematic  $Q$  dependence of the linewidth. The effect, shown in Fig. 5, could not have been caused by data mishandling during analysis and is further investigated below.

The narrow (slow) component can be ascribed to the reorientation of the whole molecule around the long axis. Assuming  $\pi$ -flips around the long axis, its  $\langle\text{FWHM}\rangle$  of 40  $\mu\text{eV}$  would correspond to the characteristic time of 131 ps which is close to the values obtained in the dielectric relaxation and NMR studies [13]. The broad (fast) one, whose width is  $Q$  dependent, clearly cannot be attributed to any single motion. Several motions could possibly contribute to this component such as (a) librations of alkyl chain elements, (b) fast conformation changes within the alkyl chains such that the molecule retains its rodlike shape (e.g., crankshaft-type  $120^\circ$ -type motions; cf. Fig. 6), on reorientation (most likely rotational diffusion) of the  $(\text{CH}_3)$  end groups. This would lead to several Lorentzian components in the spectrum [cf. Eq. (1)]. One can thus think in terms of a distribution of characteristic times rather than a number of discrete components. This is a situation well known in polymers and other highly complex disordered systems. In such systems, where characteristic times span over a wide range, the so-called “stretched exponential” approach may be successfully taken (see, e.g., Ref. [27]).

Originally developed for glass formers near the glass transition temperature, on the grounds of the mode coupling theory, the stretched-exponential concept was extended to systems showing significant distributions of correlation times. It is also frequently applied to liquid crystals and liquid crystalline polymers, especially close to the nematic-isotropic transition. In this approach, Eq. (3) takes the form

$$I'_{inc}(Q, t) \propto \exp\left[-Q^2\left(\frac{t}{\tau}\right)^\beta\right]; \quad (7)$$

hence the name. Subsequent analysis in terms of the stretched exponential provided excellent fits. The  $\beta$  param-

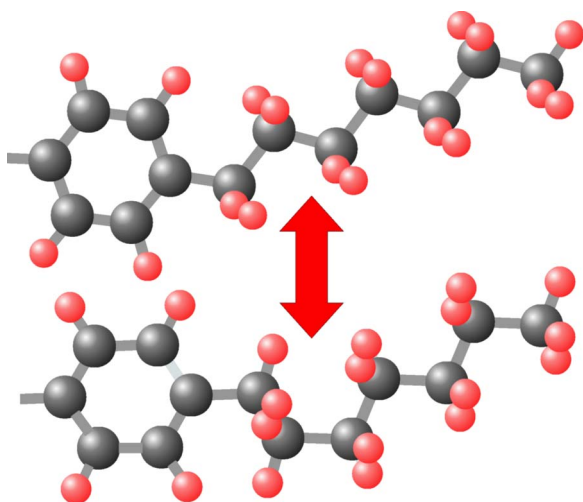


FIG. 6. (Color online) Crankshaft-type conformation changes within the right-hand side alkyl chain as simulated by “molecular mechanics” for the nematic phase. Left-hand-side chain assumed rigid for comparison and not shown in the picture. This figure also illustrates a possible “vibration-reorientation” coupling, which could also contribute to the mobility of the chain.

eter was almost  $Q$  independent, as shown in Fig. 7. Technically, data analysis in terms of the stretched-exponential intermediate scattering function, including all the least-squares fits, was performed within the framework of the MODES [25] package, mentioned above. This software environment makes use of a specific way of handling the resolution function, which allows it to operate in a Fourier-transformed space and carry out least-squares fits in the most efficient way. This is how the  $\beta$  values presented in Fig. 7 have been obtained.

The fit quality or the obtained  $\beta$  values are not affected by an inclusion or exclusion of the narrow (slow) component in the distribution.

Any significant dependence of the fitted values of the  $\beta$  parameter upon  $Q$  would obviously disqualify this approach. Consistent and meaningful values together with excellent quality fits support it. This result reinforces our original hy-

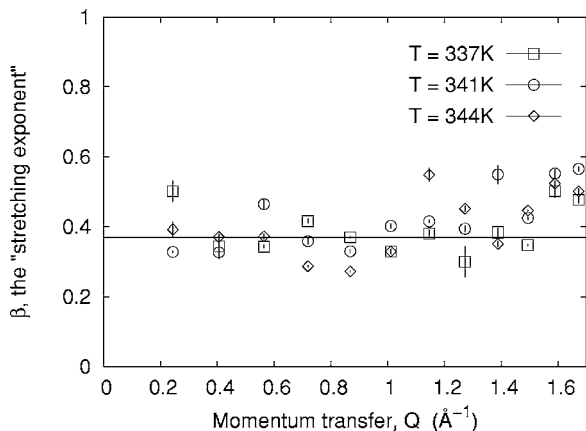


FIG. 7. The stretching exponent  $\beta$  resulting from the least-squares fits to the data, using the intermediate scattering law Eq. (7). The data presented come from nematic  $d_8$ -HAB.

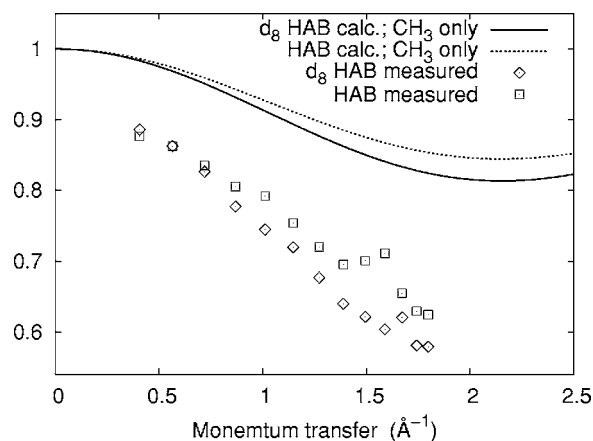


FIG. 8. The so-called quasi-EISF or apparent EISF for HAB in the crystalline phase, as compared to the “would-be” values calculated for reorienting  $\text{CH}_3$  end groups and all other hydrogen atoms frozen (immobile) within the QENS time scale.

pothesis that a number of fast reorientational motions contribute to the QENS spectra, together with the uniaxial rotational jumps of the whole molecule and/or its halves.

Finally, we recall that the preceding QENS data analysis had been carried out assuming no coupling between molecular vibrations and fast reorientation (including fast libration) within the alkyl chains. The former enter the scattering law via the Debye-Waller factor only. This standard assumption may well be questionable: by analogy, a vibration-relaxation crossover is commonly encountered in polymer systems (e.g., Refs. [28,29]).

Assuming that only the end groups reorient in the crystal phase is not enough to explain the apparent EISF as a function of  $Q$  (Fig. 8). Additional motions that can only be localized within the alkyl chains have to be accepted. This, and the above results of the stretched-exponential approach, are very strong arguments in favor of the assumption that fast reorientation within the alkyl chains takes place in such a way that the rodlike shape of the whole molecule is retained.

Another proof for this type of motion comes from the following findings by the  $^{13}\text{C}$  CPMAS NMR technique.

## B. $^{13}\text{C}$ NMR results

The isotropic chemical shifts of the various nonequivalent carbon nuclei measured from MAS spectra of anisotropic phases depend, as in liquids, upon the chemical structure, but, contrary to liquids, also on conformational and molecular packing behavior. However, unlike the corresponding chemical shifts obtained from static spectra, they do not depend on the order parameters. Moreover, other nuclear properties, such as linewidth, chemical shift anisotropy, and cross-polarization efficiency, can be directly investigated from  $^{13}\text{C}$  CPMAS spectra and can contain information on the local dynamic environment surrounding the individual carbons, due to motions of either whole molecules or fragments of them, with characteristic times in a very wide range, from nanoseconds to seconds. In this context, the comparison among the  $^{13}\text{C}$  CPMAS spectra recorded at different tem-

peratures throughout the nematic, smectic-A, and solid phases can give important information concerning the individual dynamic and conformational behavior of the aromatic core and aliphatic chains.

Typical spectra recorded in particular phases are presented in Fig. 4. The spectra recorded in the nematic phase [see Fig. 4(a)] show quite narrow aliphatic and aromatic signals, the only exception being represented by quaternary aromatic carbons, for which the signal-to-noise ratio is too small for sharp resonances to be clearly distinguished. The latter is due to poor CP efficiency that results from a combined effect of fast molecular motions involving the aromatic rings and relatively long C-H distances. The chemical shifts measured for the aliphatic carbons (14.7, 23.4, and about 30–31 ppm for C1, C2, and internal chain carbons) are typical of chains fully experiencing fast interconformational motions. In particular, the signals at 14.7 and 23.4 ppm are indicative of very fast end chains [30,31], while the 30–31 ppm peak is typical of alkyl chains performing fast jumps between *trans* and *gauche* conformations, ( $\gamma$ -*gauche* effect) [32]. It must be noticed that in our case, contrary to what happens in polyethylene or in very long alkane chains, we have a larger distribution of chemical shifts with contributions even at higher frequencies, because the chemical environment at carbon nuclei is also affected by the close aromatic moiety or end chain, given the very short, seven-term aliphatic chain.

In the smectic-A phase the spectral behavior in the aliphatic region is not substantially different from that in the nematic phase, indicating that alkyl chains do not experience a detectable reduction in their mobility. No dramatic changes can be observed even in the aromatic region, but in this case the remarkable increase in the signal-to-noise ratio suggests an increased efficiency of  $^1\text{H} \rightarrow ^{13}\text{C}$  magnetization transfer, arising from stronger dipolar interactions. This suggests that the ring-flip process begins to slow down, in agreement with the previous  $^2\text{H}$  NMR observations [13].

In the solid phase the spectrum is markedly different with respect to those in the LC phases, in both aliphatic and aromatic regions. In the latter the peaks are noticeably broadened, and the chemical shift anisotropy is greatly increased, as deduced from the spinning sideband intensities. This indicates a dramatic reduction of the mobility of the aromatic

fragments. A detectable line broadening is also observed for aliphatic resonances, which, however, preserve a good spectral resolution; the high frequency shift observed for all the carbons is indicative of a reduced interconformational mobility, with the chain tending toward an all-*trans* rigid conformation. This is particularly noticeable for internal chain carbons, the biggest signal of which now resonates at 32.2 ppm, but also for C1 and C2 carbons (respectively 15.1 and 24.2 ppm vs 14.7 and 23.4 ppm measured in the mesophases). Even though this is indicative of a clear stiffening of the alkyl chains, these values are still noticeably lower than those measured in very rigid alkyl chains (33.0–33.4 and 25.0–25.1 ppm for internal and C2 carbons, respectively) [30,31], thus clearly revealing the presence of a residual mobility affecting not only the terminal methyl group, but rather a larger portion of the chain, in agreement with QENS results.

## VI. CONCLUSIONS

A combination of two complementary experimental methods, QENS and  $^{13}\text{C}$  CPMAS, to the study of molecular dynamics in the mesogenic HAB phases brought out further information about the dynamical processes occurring in complex molecular systems. Even in the crystal phase proton motions affect the measured QENS spectra, and have to be accounted for in LC compounds. High quality of the QENS spectra allowed for a detection of fast reorientation motions within the alkyl chains together with the well known reorientation of the whole molecule or its moieties. These motions were then further elucidated by a precise  $^{13}\text{C}$  CPMAS NMR experiment. Perhaps this would not have been so exciting if we had done it the other way around, i.e., if we had confirmed NMR findings by a QENS experiment.

## ACKNOWLEDGMENTS

One of the authors (W.Z.) would like to acknowledge support from the Polish Ministry of Science and Information Society Technologies Grant No. 1 P03B 060 28. B.J.G. would like to thank OUDCE, University of Oxford, for financial assistance during the writing of this paper.

- 
- [1] P. L. Nordio, G. Rigatti, and U. Segre, *J. Chem. Phys.* **56**, 2117 (1972).
- [2] A. Kozak, J. Mościcki, and G. Williams, *Mol. Cryst. Liq. Cryst.* **201**, 1 (1991).
- [3] J. Jadżyn, C. Legrand, G. Czechowski, and D. Bauman, *Liq. Cryst.* **24**, 689 (1998).
- [4] J. Jadżyn, G. Czechowski, R. Douali, and C. Legrand, *Liq. Cryst.* **26**, 1591 (1999).
- [5] S. Urban and A. Würflinger, in *Relaxation Phenomena: Liquid Crystals, Magnetic Systems, Polymers, High- $T_c$  Superconductors, Metallic Glasses*, edited by W. Haase and S. Wróbel, (Springer-Verlag, Berlin, 2003), pp. 181–204.
- [6] A. Oka, G. Sinha, C. Glorieux, and J. Thoen, *Liq. Cryst.* **31**, 31 (2004).
- [7] R. Dong, *Nuclear Magnetic Resonance of Liquid Crystals* (Springer-Verlag, New York, 1997).
- [8] J. Dianoux and F. Volino, *J. Phys. (France)* **40**, 181 (1979).
- [9] M. Bée, *Quasielastic Neutron Scattering: Principles and Applications in Solid State Chemistry, Biology and Materials Science* (Adam Hilger IOP, Bristol, 1988).
- [10] S. Mitra, K. Venu, I. Tsukushi, S. Ikeda, and R. Mukhopadhyay, *Phys. Rev. E* **69**, 061709 (2004).
- [11] F. Volino, in *Microscopic Structure and Dynamics of Liquids*, edited by J. Dupuy and A. J. Dianoux, NATO Advanced Studies Institute Series B: Physics (Plenum Press, New York, 1978), Vol. 33, p. 221.

- [12] S. Urban, J. Czub, and B. Gestblom, *Z. Naturforsch., A: Phys. Sci.* **59**, 674 (2004).
- [13] V. Domenici, J. Czub, M. Geppi, B. Gestblom, S. Urban, and C. A. Veracini, *Liq. Cryst.* **31**, 91 (2004).
- [14] C. Forte, M. Geppi, and C. Veracini, *Z. Naturforsch., A: Phys. Sci.* **49**, 311 (1994).
- [15] D. Catalano, C. Forte, C. Veracini, J. Emsley, and G. Shilstone, *Liq. Cryst.* **2**, 345 (1987).
- [16] A. V. Zakharov and Ronald Y. Dong, *Phys. Rev. E* **63**, 011704 (2000).
- [17] A. V. Zakharov and R. Y. Dong, *Phys. Rev. E* **64**, 031701 (2001).
- [18] W. T. Coffey and Y. P. Kalmykov, *Adv. Chem. Phys.* **113**, 487 (2000).
- [19] R. Richardson, *Handbook of Liquid Crystals: Fundamentals* (Wiley VCH, Weinheim, 1998), Vol. 1, p. 680.
- [20] J. Chruściel, W. Zając, and C. Carlile, *Mol. Cryst. Liq. Cryst. Sci. Technol., Sect. A* **262**, 1649 (1995).
- [21] R. Podsiadły, J. Mayer, J. Janik, J. Krawczyk, and T. Stanek, *Acta Phys. Pol. A* **91**, 513 (1997).
- [22] D. Sivia, *Data Analysis: A Bayesian Approach* (Oxford University Press, Oxford, 1996).
- [23] J. V. der Veen, W. de Jeu, A. Grobber, and J. Boven, *Mol. Cryst. Liq. Cryst.* **17**, 291 (1972).
- [24] M. Telling and K. Andersen, *Phys. Chem. Chem. Phys.* **7**, 1255 (2005).
- [25] S. Howells, computer code MODES, ISIS Facility, RAL, [http://www.isis.rl.ac.uk/molecularspectroscopy/osiris/Modes\\_manual.pdf](http://www.isis.rl.ac.uk/molecularspectroscopy/osiris/Modes_manual.pdf).
- [26] B. Fung, A. Khitrin, and K. Ermolaev, *J. Magn. Reson.* **142**, 97 (2000).
- [27] J. Colmenero, A. Arbe, A. Alegría, M. Monkenbusch, and D. Richter, *J. Phys.: Condens. Matter* **363**, 11 (1999).
- [28] U. Buchenau, C. Schönfeld, D. Richter, *Phys. Rev. Lett.* **73**, 2344 (1994).
- [29] G. Ariedi, J.-P. Ryckaert, and D. Theodorou, *Chem. Phys.* **292**, 371 (2003).
- [30] M. Pursch, D. Vanderhart, L. Sander, X. Gu, T. Nguyen, S. Wise, and D. Gajewski, *J. Am. Chem. Soc.* **122**, 6997 (2000).
- [31] Y. Khimyak and J. Klinowski, *Phys. Chem. Chem. Phys.* **3**, 616 (2001).
- [32] A. Tonelli and F. Schilling, *Acc. Chem. Res.* **14**, 223 (1981).